

The simulated performance of c-Si/a-Si:H heterojunction solar cells with nc-Si:H, μ c-Si:H, a-SiC:H, and a-SiGe:H emitter layers

Venkanna Kanneboina

Journal of Computational Electronics

ISSN 1569-8025

J Comput Electron

DOI 10.1007/s10825-020-01626-y



Your article is protected by copyright and all rights are held exclusively by Springer Science+Business Media, LLC, part of Springer Nature. This e-offprint is for personal use only and shall not be self-archived in electronic repositories. If you wish to self-archive your article, please use the accepted manuscript version for posting on your own website. You may further deposit the accepted manuscript version in any repository, provided it is only made publicly available 12 months after official publication or later and provided acknowledgement is given to the original source of publication and a link is inserted to the published article on Springer's website. The link must be accompanied by the following text: "The final publication is available at link.springer.com".



The simulated performance of c-Si/a-Si:H heterojunction solar cells with nc-Si:H, μ c-Si:H, a-SiC:H, and a-SiGe:H emitter layers

Venkanna Kanneboina¹

Accepted: 12 November 2020

© Springer Science+Business Media, LLC, part of Springer Nature 2020

Abstract

The performance of c-Si/a-Si:H heterojunction solar cells with different emitter layers is studied by using the automat for simulation of heterostructures (AFORS-HET) tool. The a-Si:H(p) layer in the Ag/ZnO/a-Si:H(p)/a-Si:H(i)/c-Si(n)/a-Si:H(i)/a-Si:H(n)/Ag heterojunction solar cell is replaced by an nc-Si:H(p), μ c-Si:H(p), a-SiC:H(p), and a-SiGe:H(p) emitter layer. The performance of the c-Si/a-Si:H heterojunction solar cell is evaluated by varying the bandgap of these emitter layers. An open-circuit voltage (V_{oc}) of 763.3 mV, short-circuit current density (J_{sc}) of 41.89 mA/cm², fill factor (FF) of 85.61%, and efficiency (η) of 27.39% were obtained at 1.8 eV for the a-Si:H(p) emitter layer. The solar cell performance is improved by replacing the a-Si:H(p) layer with an nc-Si:H(p) layer, resulting in estimated values of 764.8 mV, 43.27 mA/cm², 85.54%, and 28.27% for V_{oc} , J_{sc} , the FF, and η , respectively, at 1.9 eV. The c-Si/a-Si:H heterojunction solar cell with the μ c-Si:H(p) emitter having a bandgap of 1.5 eV shows a good improvement in performance with V_{oc} , J_{sc} , FF, and η values of 764.8 mV, 42.75 mA/cm², 85.82%, and 28.06%, respectively. The wide bandgap and low absorption coefficient of the a-SiC:H emitter layer improve the open-circuit voltage (764.8 mV) as well as short-circuit density (42.69 mA/cm²) and thereby the efficiency (27.93%) compared with the a-Si:H(p) emitter layer. The estimated results for the c-Si/a-Si:H heterojunction solar cells having an a-SiGe:H emitter layer reveal poor performance at the low bandgap, which is improved as the bandgap of the a-SiGe:H layer is increased. The best performance with a V_{oc} of 764.8 mV, J_{sc} of 42.96 mA/cm², FF of 85.54%, and η of 28.09% at 1.7 eV is obtained for the a-SiGe:H layer.

Keywords c-Si/a-Si:H heterojunction solar cells · nc-Si:H(p) · μ c-Si:H(p) · a-SiC:H(p) · a-SiGe:H(p) · Simulation

1 Introduction

The emitter layer plays a significant role in c-Si/a-Si:H heterojunction solar cells [1–3]. This layer transmits light over a broad wavelength range to the c-Si absorber layer in order to generate free electron–hole charge carriers [3]. The use of a suitable emitter layer results in a sufficient electric field and the band bending that is required for c-Si/a-Si:H heterojunction solar cells to separate and drive the charge carriers towards the metal contacts [4, 5]. To fabricate and improve the performance of c-Si/a-Si:H heterojunction solar cells, it is important to understand and optimize the microstructure,

bandgap, thickness, doping concentration, electrical properties, etc.

For c-Si/a-Si:H heterojunction solar cells, the absorption losses at the illuminated side are a serious issue due to the high absorption coefficient of a-Si:H [1, 6]. The efficiency of c-Si/a-Si:H heterojunction solar cells can thus be improved by reducing the optical absorption losses [7]. To achieve this, materials with low absorption coefficient or a wide bandgap have been proposed for use in c-Si/a-Si:H heterojunction solar cells [8].

Several materials have been applied as the emitter layer in solar cells, including hydrogenated amorphous silicon (a-Si:H) [6, 7, 9, 10], hydrogenated nanocrystalline silicon (nc-Si:H) [11, 12], hydrogenated microcrystalline silicon (μ c-Si:H) [11, 13–15], hydrogenated amorphous silicon carbide (a-SiC:H) [14, 16–18], hydrogenated amorphous silicon germanium (a-SiGe:H) [14, 15, 18–21], etc. Other than silicon alloys, molybdenum oxide, molybdenum sulfide, and other organic materials have been also used

✉ Venkanna Kanneboina
venkanna@alumni.iitg.ac.in

¹ Department of Science and Humanities, St. Martin's Engineering College, Secunderabad, Telangana 500100, India

as the emitter layer in solar cells [22–24]. The a-Si:H has been extensively explored by many researchers due to the remarkable properties of this material [10, 25–27]. However, very few researchers have studied the use of nc-Si:H, $\mu\text{c-Si:H}$, a-SiC:H, and a-SiGe:H emitter layers in solar cells [13, 17, 19, 28–30]. These materials have been used as the emitter/window layer by increasing the optical bandgap of these materials through the addition of hydrogen atoms [31]. These hydrogen atoms improve the microstructure and reduce the coordination defects in the material [31]. However, nc-Si:H, $\mu\text{c-Si:H}$, a-SiC:H, and a-SiGe:H have mostly been used in $p-i-n$ and silicon tandem solar cells but very less in c-Si/a-Si:H heterojunction solar cells [4, 19, 32].

In 1983, Okuda et al. first reported a-Si/poly c-Si heterojunction solar cell, with efficiency of 12% [33]. In 1992, researchers at Sanyo developed a new c-Si/a-Si:H heterojunction (HIT) solar cell technology, achieving a high efficiency value of 18.1% [34]. After this, record efficiency was reported by Sanyo based on a breakthrough Si photovoltaic technology, many research groups were attracted towards working on c-Si/a-Si:H heterojunction solar cells [1, 35]. In 2014, Sanyo reported the highest efficiency of 25.6% [6] with an open-circuit voltage of 750 mV on n -type c-Si substrates using the heterojunction with intrinsic thin layer (HIT) solar cell structure [7]. At present, the highest reported efficiency is 26.7% on n -type [36, 37] and 26.1% on p -type c-Si wafers, using interdigitated back-contact silicon heterojunction (IBC-SHJ) solar cell technology [38]. Solar cells based on amorphous silicon with efficiency of 8–10% are reported in literature with a-Si:H emitter [39]. Efficiency values of 11.9%, 12.7%, and 14% have been reported for microcrystalline silicon, a-Si/nc-Si, and a-Si/nc-Si/nc-Si thin-film solar cells [39], whereas 12.3% has been reported for a-Si/nc-Si tandem solar cells [39]. However, a large number of processing parameters, such as the thickness, doping, and bandgap of the a-Si:H and TCO layers as well as metal contacts must be optimized to fabricate c-Si/a-Si:H heterojunction solar cells. It is a huge task to study the effect of each parameter on the solar cell performance experimentally.

As the efficiency of solar cells has been improved, many researchers have worked on simulations of solar cells. The results have been implemented to improve the performance. Many researchers have designed different structures and studied the effect of varying the thickness of the layers, the bandgap, the interface defect states, and the doping concentration [4, 40, 41]. Antwi et al. achieved a simulated efficiency of 29.19% by optimizing the defect density and fixed interface charges [42]. Dwivedi et al. achieved a simulated efficiency of 27% by designing layers with different thicknesses in various structures [10]. Arti et al. reported a high efficiency value of 24.14% for c-Si/ $\mu\text{c-Si:H}$ heterojunction solar cells [43]. Efficiency values of 9.35% and 17% have been reported for a-Si:H/nc-Si:H and $\mu\text{c-Si:H}$ thin-film solar

cells, respectively, based on simulations [12, 13]. Efficiency values of 15% and 17% have been reported for a-Si:H/ $\mu\text{c-Si:H}$ and a-SiCH/a-SiGe:H/ $\mu\text{c-Si:H}$ thin-film solar cells, respectively [15]. The incorporation of carbon atoms into the Si network can improve the performance of different type of solar cells, with a reported value of 10% for a-SiC:H/a-Si:H/a-SiGe:H solar cells [18]. Some research groups have compared simulation and experimental results for different types of solar cells [29, 40, 44, 45]. It is observed that experimental results are closely comparable to simulated results for solar cells.

Simulation tools can provide enhanced understanding of the effects of material properties on the performance of solar cells without high costs in terms of investment, risk, and time. AFORS-HET is one of the best simulation tools to study c-Si/a-Si:H heterojunction solar cells [27, 46–50]. We have used primarily optimized device results from simulations to fabricate single-sided c-Si/a-Si:H heterojunction solar cells experimentally [51]. Initially, we analyze how deposition parameters such as the doping density, thickness, bandgap, interface defect density, etc. affect the device performance and understand the different conditions for device fabrication to improve the efficiency.

In this work, the performance of c-Si/a-Si:H heterojunction solar cells is studied using different emitter layers made of a-Si:H, nc-Si:H, $\mu\text{c-Si:H}$, a-SiC:H, and a-SiGe:H, by applying the AFORS-HET simulation tool. The bandgap of each emitter layer is varied to study and improve the performance of the c-Si/a-Si:H heterojunction solar cells.

2 Simulation details

The AFORS-HET tool is used to model c-Si/a-Si:H heterojunction solar cells. Solar radiation with the AM1.5 spectrum at a power density of 100 mW/cm² together with flat-band metal contacts are used in the simulations. The input parameters for the c-Si/a-Si:H heterojunction solar cells are presented in Table 1. The density of states distribution for all the layers is taken from standard references [4, 5, 10, 11, 28, 46, 52, 53]. The other parameters are set based on the preset values in the AFORS-HET software [10, 27].

A schematic diagram of the c-Si/a-Si:H heterojunction solar cell structure is shown in Fig. 1. The a-Si:H(p) layer is replaced by emitter layers made of different materials, viz. nc-Si:H(p), $\mu\text{c-Si:H}$ (p), a-SiC:H(p), and a-SiGe:H(p) in the c-Si/a-Si:H structure shown in Fig. 1. The bandgap of the different emitter layers is varied to evaluate its effect on the performance of the solar cell. The thickness of all the a-Si:H, nc-Si:H(p), $\mu\text{c-Si:H}$ (p), a-SiC:H(p), and a-SiGe:H(p) layers was kept at 5 nm. A schematic band-bending diagram of the c-Si/a-Si:H heterojunction solar cells is shown in Fig. 2.

Table 1 The values of the input parameters used in the presented simulations of c-Si/a-Si:H heterojunction solar cells

Parameter	c-Si(<i>n</i>)	a-Si:H(<i>n</i>)	a-Si:H(<i>i</i>)	a-Si:H(<i>p</i>)	nc-Si:H(<i>p</i>)	μc-Si:H(<i>p</i>)	a-SiC:H(<i>p</i>)	a-SiGe:H(<i>p</i>)
Thickness	250 μm	5 nm	5 nm	5 nm	5 nm	5 nm	5 nm	5 nm
Dielectric constant	11.1	11.1	11.1	11.1	11.9	11.9	11.9	14
Electron affinity (eV)	4.05	3.9	3.9	3.9	3.9	3.9	3.9	4.01
Bandgap (eV)	1.12	1.72	1.72	Variable	Variable	Variable	Variable	Variable
Effective conduction-band density (cm ⁻³)	2.8 × 10 ¹⁹	6.9 × 10 ²⁰	6.9 × 10 ²⁰	6.9 × 10 ²⁰	3.0 × 10 ¹⁹	3.0 × 10 ¹⁹	2.5 × 10 ²⁰	1.0 × 10 ²⁰
Effective valence-band density (cm ⁻³)	2.8 × 10 ¹⁹	1.2 × 10 ²¹	1.2 × 10 ²¹	1.2 × 10 ²¹	3.0 × 10 ¹⁹	3.0 × 10 ¹⁹	2.5 × 10 ²⁰	1.0 × 10 ²⁰
Electron mobility (cm ² V ⁻¹ s ⁻¹)	1321	7	7	7	60	50	10	60
Hole mobility (cm ² V ⁻¹ s ⁻¹)	461	1	1	1	4	5	1	10
Acceptor concentration (cm ⁻³)	0	0	0	6.1 × 10 ²¹	3.0 × 10 ¹⁹	1.0 × 10 ¹⁹	3.0 × 10 ²⁰	1 × 10 ¹⁹
Donor concentration (cm ⁻³)	5 × 10 ¹⁶	1.7 × 10 ²¹	0	0	0	0	0	0
Thermal velocity of electrons (cm s ⁻¹)	10 ⁷	10 ⁷	10 ⁶	10 ⁷	10 ⁷	10 ⁷	10 ⁷	10 ⁷
Thermal velocity of holes (cm s ⁻¹)	10 ⁷	10 ⁷	10 ⁶	10 ⁷	10 ⁷	10 ⁷	10 ⁷	10 ⁷
Layer density (g cm ⁻³)	2.328	2.328	2.328	2.328	2.328	2.328	2.328	2.328

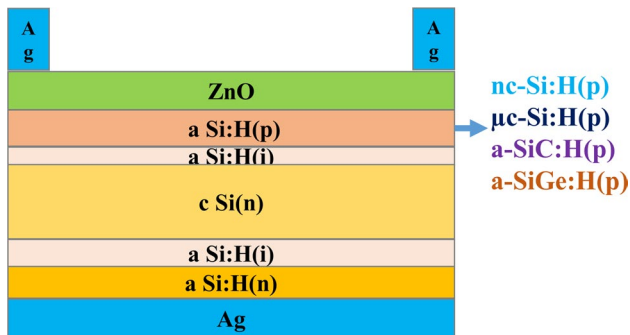


Fig. 1 A schematic of the structure of the c-Si/a-Si:H heterojunction solar cells

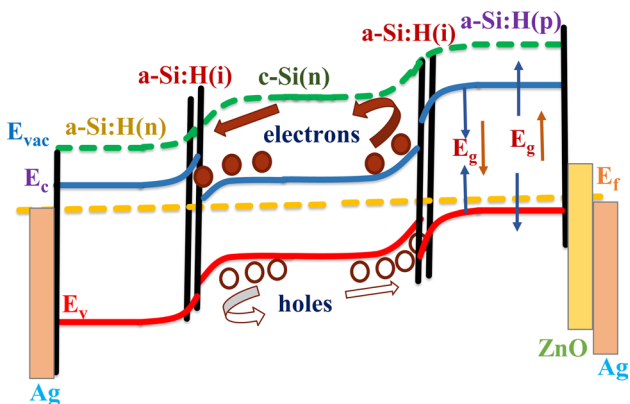


Fig. 2 A band-bending diagram of the c-Si/a-Si:H heterojunction solar cells with decreasing ($E_g\downarrow$) and increasing ($E_g\uparrow$) bandgap of the emitter layer

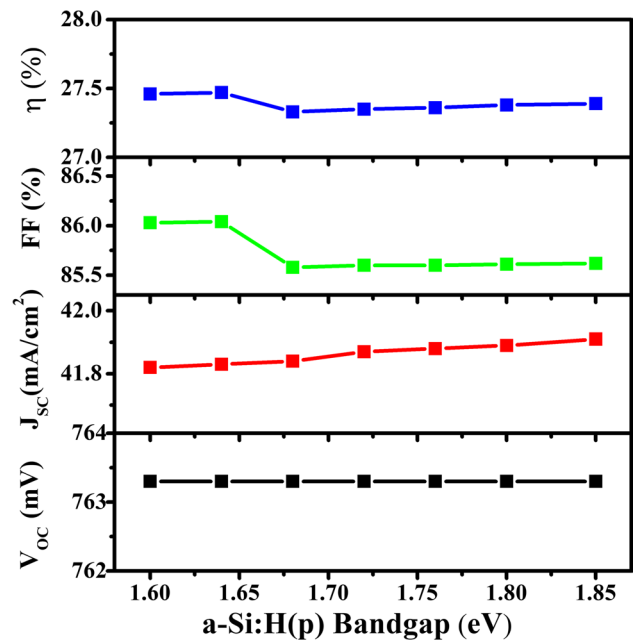


Fig. 3 The solar cell parameters as functions of the bandgap of the a-Si:H(*p*) emitter layer

3 Results and discussion

3.1 The c-Si/a-Si:H heterojunction solar cell with an a-Si:H(*p*) emitter layer

Figure 3 shows the solar cell parameters as a function of the bandgap of the a-Si:H(*p*) emitter layer. The optical bandgap of the a-Si:H(*p*) layer is varied from 1.6 to 1.85 eV in steps of 0.04 eV, and the solar cell parameters

V_{oc} , J_{sc} , FF, and η are estimated. The range of bandgap values of the emitter layer used in the simulations is closely comparable to the values of experimentally deposited a-Si:H films. The thickness of all the a-Si:H layers is kept constant of 5 nm. The bandgap of the a-Si:H(i) and a-Si:H(n) layer is fixed at 1.72 eV. The open-circuit voltage is constant in the energy range from 1.6 to 1.85 eV. The J_{sc} values increase from 41.82 to 41.91 mA/cm² as the bandgap of the emitter layer is increased. High FF values of 86.03% and 86.04% are observed at 1.6 and 1.64 eV, respectively, but the FF decreases at 1.68 eV and then increases slightly with further increase in the bandgap. An FF value of 85.61% is observed at 1.8 eV for the a-Si:H(p) layer. As a result, an efficiency of 27.47% is obtained at 1.64 eV, decreasing to 27.33%. An efficiency of 27.38% is observed at 1.8 eV for the p-layer. A high efficiency is observed at 1.64 eV for the a-Si:H(p) layer, but the efficiency value is reported for a bandgap of 1.8 eV, since this is the value reported experimentally for a-Si:H films. An efficiency of 27.47% is obtained at 1.64 eV, but it then decreases slightly to 27.38% at 1.8 eV; That is, the efficiency increases slightly initially but then decreases. This could be due to the greater number of photons allowed to enter the c-Si wafer to generate free electron–hole pairs through the emitter layer when the bandgap of the emitter layer is low, which results in the efficiency improvement. With a slight increase in the bandgap, some of the photons are absorbed by the emitter layer, resulting in a reduction in the photocurrent.

3.2 The c-Si/a-Si:H heterojunction solar cells with an nc-Si:H(p) emitter layer

Hydrogenated nanocrystalline silicon (nc-Si:H) has a large bandgap value, lower defect density, and higher conductivity compared with a-Si:H films. These properties make nc-Si:H(p) a suitable material for the emitter layer in c-Si/a-Si:H heterojunction solar cells. The high bandgap and less-defective nature of this emitter layer improve the short-circuit density and open-circuit voltage, respectively [3, 54]. Figure 4 shows the solar cell parameters as function of the bandgap of the nc-Si:H(p) layer. The bandgap of the nc-Si:H(p) is varied from 1.78 to 1.9 eV, and the V_{oc} , J_{sc} , FF, and η of the solar cells are estimated. V_{oc} does not change as the bandgap is increased in the range of 1.78–1.9 eV. The observed V_{oc} (764.8 mV) is about 1.5 mV higher than that obtained (763.3 mV) with the a-Si:H(p) emitter layer, since the defect density in the bulk and on the surface of the nc-Si:H as well as at the interface is lower compared with a-Si:H(p). J_{sc} improves as the bandgap of the p-layer is increased. It is observed that J_{sc} improves even at a low bandgap of 1.78 eV for the nc-Si:H(p) layer. J_{sc} is enhanced by about 2 mA/cm² as compared with the a-Si:H(p) emitter

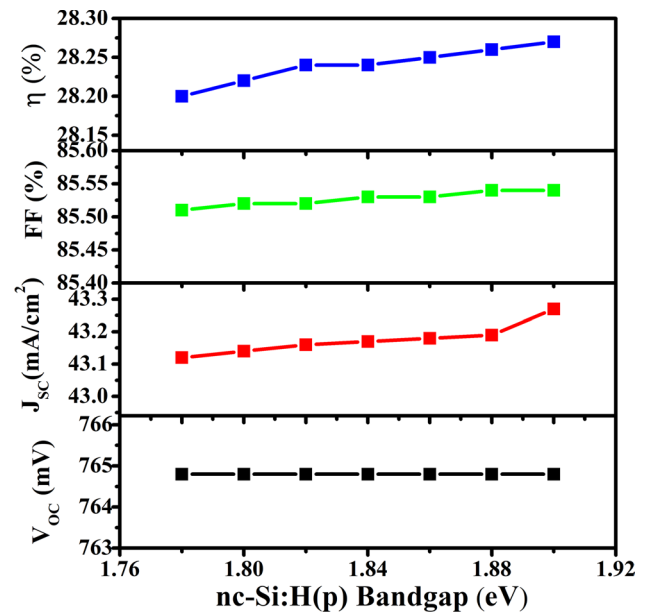


Fig. 4 The solar cell parameters as functions of the bandgap of the nc-Si:H(p) emitter layer

layer. A high J_{sc} value of 43.27 mA/cm² is obtained with the nc-Si:H layer having a bandgap of 1.9 eV. This can be attributed to the fact that the high-bandgap emitter allows the transmission of high-energy photons to be absorbed in the c-Si and thus generate a large number of electron–hole pairs. The other reason is that the electrical conductivity of the nc-Si:H(p) is higher than that of the a-Si:H(p) layer. The FF value does not change as the bandgap is increased, while the efficiency increases. A high efficiency value of 28.27% is observed for the nc-Si:H(p) layer with a bandgap of 1.9 eV.

3.3 The c-Si/a-Si:H heterojunction solar cells with a μ c-Si:H(p) emitter layer

Hydrogenated microcrystalline silicon (μ c-Si:H) is one of the prominent materials for fabrication of solar cells. Its remarkable properties such as high conductivity, lower coordination defect density, low absorption coefficient, and suitable bandgap make μ c-Si:H(p) applicable as the emitter layer in solar cells [4, 54]. Figure 5 shows the V_{oc} , J_{sc} , FF, and η values of the solar cells as a function of the bandgap of the μ c-Si:H(p) layer, revealing low values of 739.8 mV, 42.64 mA/cm², 79.78%, and 25.17%, respectively, at 1.25 eV. The V_{oc} increases from 739.8 mV to 763.3 mV in the range from 1.25 to 1.35 eV, respectively. At 1.4 eV, V_{oc} increases to 764.8 mV but saturates with further increase in the bandgap of the μ c-Si:H(p) layer. J_{sc} increases continuously from 42.64 to 42.78 mA/cm² as the bandgap of the p-layer is increased in the range from 1.25 to 1.55 eV. The FF increases from 79.78% to 85.82% as the bandgap is

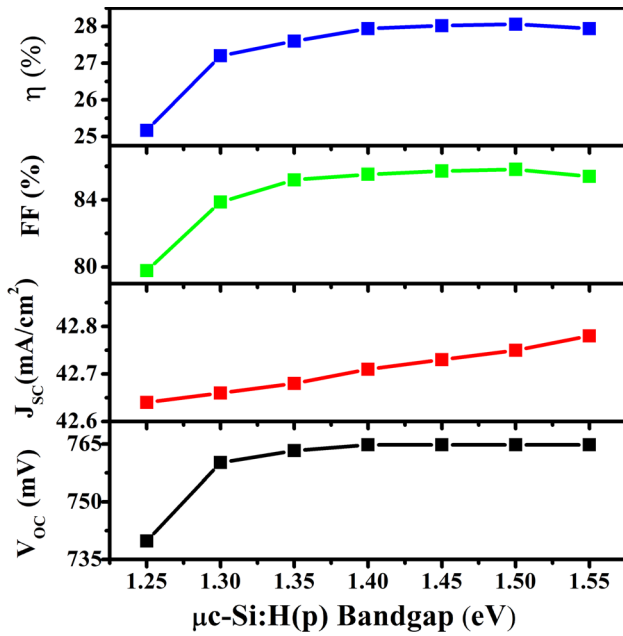


Fig. 5 The solar cell parameters as functions of the bandgap of the $\mu\text{c-Si:H}(p)$ emitter layer

increased from 1.25 to 1.5 eV but then decreases to 85.41% at 1.55 eV. A maximum FF value of 85.82% is found at 1.5 eV for the $\mu\text{c-Si:H}(p)$ layer. A low efficiency of 25.17% is observed at 1.25 eV. This efficiency increases as the bandgap of the emitter layer is increased, reaching 28.06% at 1.5 eV, after which η decreases to 27.94% when the bandgap of the p -layer is 1.55 eV. For low bandgap values, the majority carriers from $c\text{-Si}(n)$ can easily enter the $\mu\text{c-Si:H}(p)$ and recombine, resulting in a low open-circuit voltage of the solar cell. As the bandgap of the $\mu\text{c-Si:H}(p)$ is increased, the majority carrier electrons in the $c\text{-Si}(n)$ see a high barrier height to enter the $\mu\text{c-Si:H}(p)$ layer and thus move towards the backside $a\text{-Si:H}(n)$ layer, resulting in a significant reduction in the recombination losses. This leads to an improvement in the V_{oc} and thereby the efficiency of the $c\text{-Si}/a\text{-Si:H}$ heterojunction solar cells.

3.4 The $c\text{-Si}/a\text{-Si:H}$ heterojunction solar cells with an $a\text{-SiC:H}(p)$ emitter layer

Hydrogenated amorphous silicon carbide ($a\text{-SiC:H}$) is very useful as a window layer for solar cells. This window layer transmits the maximum number of incident photons to allow them to reach the $c\text{-Si}$ wafer and thus generate free charge carriers. Indeed, $a\text{-SiC:H}$ has a wide bandgap, high electrical conductivity, high mobility, and low absorption coefficient [4, 31, 55]. The $a\text{-SiC:H}$ layer is formed by adding carbon atoms to the $a\text{-Si:H}$ network. The $a\text{-SiC:H}$ layer also fixes the lattice mismatch between the transparent conducting

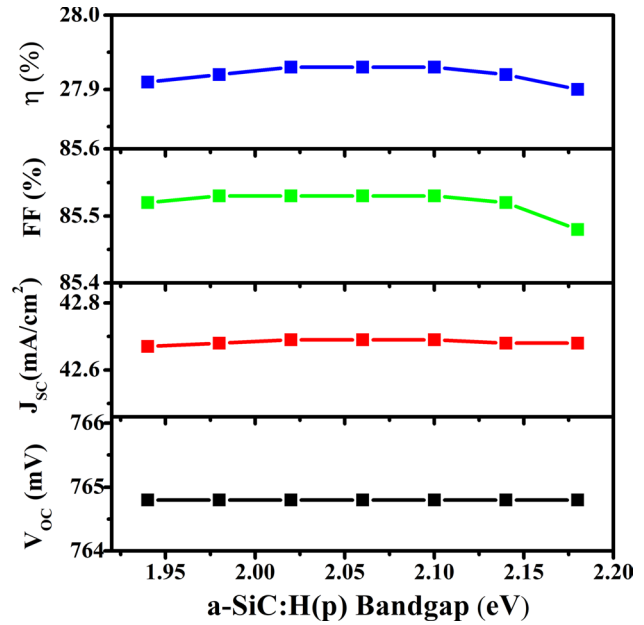


Fig. 6 The solar cell parameters as functions of the bandgap of the $a\text{-SiC:H}(p)$ emitter layer

oxide (ZnO) and the intrinsic $a\text{-Si:H}$ layer. The wide bandgap of the $a\text{-SiC:H}$ layer also adjusts the band discontinuity between the valance band and conduction band. The variation of the solar cell parameters V_{oc} , J_{sc} , FF, and η is plotted as a function of the bandgap of the $a\text{-SiC:H}(p)$ emitter layer in the range of 1.94–2.18 eV in Fig. 6. V_{oc} does not change and remains constant in this energy range. However, V_{oc} is enhanced by about 1.5 mV when using $a\text{-SiC:H}(p)$ compared with $a\text{-Si:H}(p)$, due to the reduced recombination density in the $a\text{-SiC:H}(p)$ layer. J_{sc} does not change significantly, and a high value of J_{sc} is observed in the range of 2.02–2.1 eV. The J_{sc} values are improved by about 1 mA/cm² compared with the $a\text{-Si:H}(p)$ layer, due to the wider bandgap and low absorption coefficient of the $a\text{-SiC:H}(p)$ layer. The FF values increase initially but then decrease at 2.14 and 2.18 eV for the $a\text{-SiC:H}(p)$ layer. The best values of the FF (85.53%) and η (27.93%) are observed at 2.1 eV for the $a\text{-SiC:H}(p)$ emitter layer. In the case of $a\text{-SiC:H}$, the band discontinuity (barrier) increases as the bandgap of the layer is increased, which leads to recombination losses of charge carriers as well as the absorption of photons by the emitter layer. This could be the reason for the decrease in the efficiency of the $c\text{-Si}/a\text{-Si:H}$ solar cells with the $a\text{-SiC:H}$ emitter layer at a high bandgap.

3.5 The $c\text{-Si}/a\text{-Si:H}$ heterojunction solar cells with an $a\text{-SiGe:H}(p)$ emitter layer

Hydrogenated amorphous silicon germanium ($a\text{-SiGe:H}$) is prepared by adding germanium (Ge) atoms to the $a\text{-Si:H}$

network. However, Ge material is not easily available and is also expensive. Germanium can be used in many electronic devices due to its low bandgap, which allows the absorption of broad spectral range. The bandgap of a-SiGe can be increased by adding hydrogen atoms into its structure. However, very few researchers have focused on a-SiGe:H material. Understanding the optical, structural, and electrical properties of a-SiGe:H is therefore of great significance. In this work, the bandgap of a-SiGe:H is varied from 1.1 to 1.7 eV to study the effect on the performance of the solar cells by estimating the V_{oc} , J_{sc} , FF, and η values (Fig. 7). Low V_{oc} , FF, and efficiency values of 628.9 mV, 77.95%, and 20.26%, respectively, are obtained for a-SiGe:H with a bandgap of 1.1 eV. However, V_{oc} , J_{sc} , FF, and η increase to 714.8 mV, 41.4 mA/cm², 82.19%, and 24.33%, respectively, at 1.2 eV. The performance of the solar cell is improved as the bandgap of the a-SiGe:H emitter layer is increased. The V_{oc} , J_{sc} , FF, and η are enhanced to 758.6–763.3 mV, 41.6–42.38, 85.26–85.57, and 26.91–27.68% in the range of 1.3–1.5 eV, respectively. The estimated V_{oc} saturates at 764.8 mV, and J_{sc} , FF, and η values of 42.81 and 42.94 mA/cm², 85.5 and 85.54%, and 27.99 and 28.09% are found for the a-SiGe:H(p) layer with a bandgap of 1.6 and 1.7 eV, respectively. It is found that a-SiGe:H with a large bandgap can be used as the emitter layer to improve the performance of the c-Si/a-Si:H heterojunction solar cells.

These results indicate that the performance of the c-Si/a-Si:H heterojunction cells is improved by using the nc-Si:H(p), μ c-Si:H(p), a-SiC:H(p), and a-SiGe:H(p) emitter

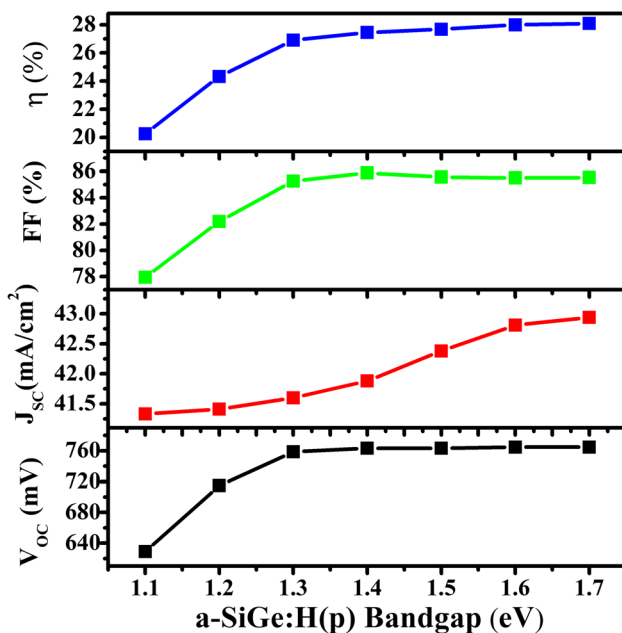


Fig. 7 The solar cell parameters as functions of the bandgap of the a-SiGe:H(p) emitter layer

layers. The high absorption coefficient, high defect density, and low conductivity of the a-Si:H(p) layer deteriorate the performance of the solar cell. In the case of the nc-Si:H(p) layer, the efficiency is improved due to the lower level of coordination defects, high bandgap, high conductivity, and improved microstructure of the nc-Si:H(p) layer. The wider bandgap and low absorption coefficient of the a-SiC:H(p) layer increase the short-circuit current density and open-circuit voltage, as the wider bandgap of the a-SiC:H(p) allows more light to reach the c-Si(n) and thus generate a large number of free charge carriers, while also reducing the recombination losses. It is observed that the solar cells with a μ c-Si:H(p) or a-SiGe:H emitter layer show poor performance for low bandgaps due to charge carrier recombination, although their performance improves as the bandgap of the μ c-Si:H(p) and a-SiGe:H layer is increased. The estimated results suggest that emitter layers with a high bandgap, high conductivity, and lower defect density are required to achieve c-Si/a-Si:H heterojunction solar cells with the best performance.

4 Conclusions

Ag/ZnO/a-Si:H(p)/a-Si:H(i)/c-Si(n)/a-Si:H(i)/a-Si:H(n)/Ag solar cells are designed and evaluated using the AFORS-HET simulation tool. The a-Si:H(p) layer in the c-Si/a-Si:H heterojunction solar cell is replaced by an nc-Si:H(p), μ c-Si:H(p), a-SiC:H(p), or a-SiGe:H(p) emitter layer. The performance of the c-Si/a-Si:H heterojunction solar cell is evaluated by varying the bandgap of these emitter layers. The best values of the open-circuit voltage (V_{oc}) (763.3 mV), short-circuit current density (J_{sc}) (41.89 mA/cm²), fill factor (FF) (85.61%), and efficiency (η) (27.39%) are obtained when using the a-Si:H(p) layer with a bandgap of 1.8 eV, which is closely comparable to the experimental value for a-Si:H film. It is found that the performance of the solar cell can be improved by replacing the a-Si:H(p) with an nc-Si:H(p) layer, resulting in estimated values of 764.8 mV, 43.27 mA/cm², 85.54%, and 28.27% for V_{oc} , J_{sc} , the FF, and η , respectively, for the nc-Si:H(p) layer with a bandgap of 1.9 eV. This improvement in the performance of the c-Si/a-Si:H heterojunction solar cells results from the improved microstructure, high conductivity, and low defect density of the nc-Si:H(p) layer. The estimated values of V_{oc} , J_{sc} , the FF, and η are 764.8 mV, 42.75 mA/cm², 85.82%, and 28.06%, respectively, for the c-Si/a-Si:H heterojunction solar cell with a μ c-Si:H(p) emitter layer having a bandgap of 1.5 eV. The observed enhancement in the performance is due to the reduced recombination losses resulting from the increased bandgap of the μ c-Si:H(p) layer. The open-circuit voltage (764.8 mV) as well as the short-circuit density (42.69 mA/cm²) and thereby efficiency (27.93%) are

improved by the wide bandgap and low absorption coefficient of the a-SiC:H(*p*) emitter layer compared with the a-Si:H(*p*) layer. It is observed that the solar cells with an a-SiGe:H(*p*) emitter layer show poor performance at low bandgap values, which is improved as the bandgap of the a-SiGe:H layer is increased. The best values obtained with the a-SiGe:H layer are a V_{oc} of 764.8 mV, J_{sc} of 42.96 mA/cm², FF of 85.54%, and η of 28.09%, at 1.7 eV. It is found that emitter layers with a high bandgap, high conductivity, and lower defect density are required to obtain c-Si/a-Si:H heterojunction solar cells with the best performance. These findings really help and encourage experimental researchers to optimize the properties of such layers to potentially design and fabricate solar cell devices and improve their performance without high costs in terms of time and money.

Acknowledgements The authors acknowledge Helmholtz-Zentrum Berlin for providing the AFORS-HET simulation software.

References

- De Wolf, S., Descoedres, A., Holman, Z.C., Ballif, C.: High-efficiency silicon heterojunction solar cells: a review. *Green* **2**, 7–24 (2012). <https://doi.org/10.1515/green-2011-0018>
- Ramanujam, J., Verma, A.: Photovoltaic properties of a-Si:H films grown by plasma enhanced chemical vapor deposition: a review. *Mater. Express* **2**, 177–196 (2012). <https://doi.org/10.1166/mex.2012.1073>
- Wilfried, G.J., van Sark, H.M., Korte, L.: *Physics and Technology of Amorphous-Crystalline Heterojunction Silicon Solar Cells*. Springer (2012). <https://doi.org/10.1007/978-3-642-22275-7>
- Schropp, R.E.I., Zeman, M.: *Amorphous and Microcrystalline Silicon Solar Cells: Modeling, Materials and Device Technology*. Kluwer, Dordrecht (1998)
- Fonash, S.J.: *Solar Cell Device Physics*. Elsevier, Amsterdam (2010). [https://doi.org/10.1016/0025-5408\(82\)90173-8](https://doi.org/10.1016/0025-5408(82)90173-8)
- Masuko, K., Shigematsu, M., Hashiguchi, T., Fujishima, D., Kai, M., Yoshimura, N., Yamaguchi, T., Ichihashi, Y., Mishima, T., Matsubara, N., Yamanishi, T., Takahama, T., Taguchi, M., Maruyama, E., Okamoto, S.: Achievement of more than 25% conversion efficiency with crystalline silicon heterojunction solar cell. *IEEE J. Photovolt.* **4**, 1433–1435 (2014). <https://doi.org/10.1109/JPHOTOV.2014.2352151>
- Taguchi, M., Yano, A., Tohoda, S., Matsuyama, K., Nakamura, Y., Nishiwaki, T., Fujita, K., Maruyama, E.: 24.7% Record efficiency HIT solar cell on thin silicon wafer. *IEEE J. Photovolt.* **4**, 96–99 (2014). <https://doi.org/10.1109/JPHOTOV.2013.2282737>
- Huang, H., Tian, G., Zhou, L., Yuan, J., Fahrner, W.R., Zhang, W., Li, X., Chen, W., Liu, R.: Simulation and experimental study of a novel bifacial structure of silicon heterojunction solar cell for high efficiency and low cost. *Chin. Phys. B* (2018). <https://doi.org/10.1088/1674-1056/27/3/038502>
- Kanneboina, V., Madaka, R., Agarwal, P.: High open circuit voltage c-Si/a-Si:H heterojunction solar cells: influence of hydrogen plasma treatment studied by spectroscopic ellipsometry. *Sol. Energy* **166**, 255–266 (2018a). <https://doi.org/10.1016/j.solener.2018.03.068>
- Dwivedi, N., Kumar, S., Bisht, A., Patel, K., Sudhakar, S.: Simulation approach for optimization of device structure and thickness of HIT solar cells to achieve ~27% efficiency. *Sol. Energy* **88**, 31–41 (2013). <https://doi.org/10.1016/j.solener.2012.11.008>
- Ide, Y., Saito, Y., Yamada, A., Konagai, M.: 2-Step growth method and microcrystalline silicon thin film solar cells prepared by hot wire cell method. *Jpn. J. Appl. Phys.* **43**, 2419–2424 (2004). <https://doi.org/10.1143/JJAP.43.2419>
- Belfar, A.: Simulation study of the a-Si:H/nc-Si:H solar cells performance sensitivity to the TCO work function, the band gap and the thickness of i-a-Si:H absorber layer. *Sol. Energy* **114**, 408–417 (2015). <https://doi.org/10.1016/j.solener.2015.02.010>
- Sharma, M., Kumar, S., Dwivedi, N., Juneja, S., Gupta, A.K., Sudhakar, S., Patel, K.: Optimization of band gap, thickness and carrier concentrations for the development of efficient microcrystalline silicon solar cells: a theoretical approach. *Sol. Energy* **97**, 176–185 (2013). <https://doi.org/10.1016/j.solener.2013.08.012>
- Fantoni, A., Vieira, M., Martins, R.: Simulation of hydrogenated amorphous and microcrystalline silicon optoelectronic devices. *Math. Comput. Simul.* **49**, 381–401 (1999). [https://doi.org/10.1016/s0378-4754\(99\)00055-5](https://doi.org/10.1016/s0378-4754(99)00055-5)
- Zeman, M., Krc, J.: Optical and electrical modeling of thin-film silicon solar cells. *J. Mater. Res.* **23**, 889–898 (2008). <https://doi.org/10.1557/jmr.2008.0125>
- Madaka, R., Kanneboina, V., Agarwal, P.: Enhanced performance of amorphous silicon solar cells (110°C) on flexible substrates with a-SiC:H(*p*) window layer and H₂ plasma treatment at *n/i* and *i/p* interface. *Semicond. Sci. Technol.* **33**, 3 (2018)
- Shao, Q.Y., Chen, A.Q., Zhu, K.G., Zhang, J.: Numerical simulation of a P + a-SiC:H/N + poly-Si solar cell with high efficiency and fill factor. *Chin. Phys. Lett.* (2012). <https://doi.org/10.1088/0256-307X/29/8/087302>
- Chang, S.T., Tang, M., He, R.Y., Wang, W.C., Pei, Z., Kung, C.Y.: TCAD simulation of hydrogenated amorphous silicon-carbon/microcrystalline-silicon/hydrogenated amorphous silicon-germanium PIN solar cells. *Thin Solid Films* **518**, S250–S254 (2010). <https://doi.org/10.1016/j.tsf.2009.10.100>
- Abuzairi, T., Raden Poespawati, N.: A simple optimization of triple-junction solar cell nc-Si:H/a-Si:H/a-SiGe:H using computer modeling and robust design. *Adv. Mater. Res.* **896**, 455–458 (2014). <https://doi.org/10.4028/www.scientific.net/AMR.896.455>
- Soukup, R.J., Ianno, N.J., Darveau, S.A., Exstrom, C.L.: Thin films of a-SiGe:H with device quality properties prepared by a novel hollow cathode deposition technique. *Sol. Energy Mater. Sol. Cells* **87**, 87–98 (2005). <https://doi.org/10.1016/j.solmat.2004.08.023>
- Yan, B., Zhao, L., Zhao, B., Chen, J., Wang, G., Diao, H., Wang, W.: High-performance a-SiGe:H thin film prepared by plasma-enhanced chemical vapor deposition with high plasma power for solar-cell application. *Phys. Status Solidi Appl. Mater. Sci.* **209**, 2527–2531 (2012). <https://doi.org/10.1002/pssa.201228281>
- Battaglia, C., Wolf, S. De, Yin, X., Zheng, M., Ballif, C., Javey, A., Division, M.S., Berkeley, L., Film, T., Polytechnique, E., Lausanne, F. De: Hole selective MoOx contact for silicon heterojunction solar cells. In: 2014 IEEE 40th Photovoltaic Specialist Conference (PVSC), pp. 968–970 (2014)
- Wu, W., Bao, J., Liu, Z., Lin, W., Yu, X., Cai, L., Liu, B.: Multi-layer MoOx/Ag/MoOx emitters in dopant-free silicon solar cells. *Mater. Lett.* **189**, 86–88 (2017). <https://doi.org/10.1016/j.matlet.2016.11.059>
- Xu, S., Zeng, X., Wang, W., Zhou, G., Hu, Y., Wu, S., Zeng, Y.: Simulation and optimization characteristic of novel MoS₂/c-Si HIT solar cell. *J. Miner. Mater. Charact. Eng.* **05**, 323–338 (2017). <https://doi.org/10.4236/jmmce.2017.55027>
- Procel, P., Yang, G., Isabella, O., Zeman, M.: Theoretical evaluation of contact stack for high efficiency IBC-SHJ solar cells. *Sol. Energy Mater. Sol. Cells* **186**, 66–77 (2018). <https://doi.org/10.1016/j.solmat.2018.06.021>

26. Morales-Acevedo, A., Hernández-Como, N., Casados-Cruz, G.: Modeling solar cells: A method for improving their efficiency. *Mater. Sci. Eng. B* **177**, 1430–1435 (2012). <https://doi.org/10.1016/j.mseb.2012.01.010>
27. Varache, R., Leendertz, C., Gueunier-Farret, M.E., Haschke, J., Muñoz, D., Korte, L.: Investigation of selective junctions using a newly developed tunnel current model for solar cell applications. *Sol. Energy Mater. Sol. Cells* **141**, 14–23 (2015). <https://doi.org/10.1016/j.solmat.2015.05.014>
28. Iftiqar, S.M., Park, H., Kim, S., Yi, J.: Theoretical investigation of transparent front surface field layer on the performance of heterojunction silicon solar cell. *Sol. Energy Mater. Sol. Cells* **204**, 110238 (2020). <https://doi.org/10.1016/j.solmat.2019.110238>
29. Qiu, D., Duan, W., Lambertz, A., Bittkau, K., Steuter, P., Liu, Y., Gad, A., Pomaska, M., Rau, U., Ding, K.: Front contact optimization for rear-junction SHJ solar cells with ultra-thin n-type nanocrystalline silicon oxide. *Sol. Energy Mater. Sol. Cells* **209**, 110471 (2020). <https://doi.org/10.1016/j.solmat.2020.110471>
30. Azizi, T., Torchani, A., Ben Karoui, M., Gharbi, R., Fathallah, M., Tresso, E.: Effect of defects on the efficiency of a-Si:C:H p-i-n based solar cells. In: 2013 International Conference on Electrical Engineering and Software Applications, ICEESA 2013. pp. 1–5 (2013)
31. Street, R.A.: *Hydrogenated Amorphous Silicon*. Cambridge University Press, Cambridge (1991)
32. Shan, F., Wei, W.: Design and simulation of a-Si:H/nc-Si:H tandem solar cells. *Adv. Mater. Res.* **382**, 100–105 (2012). <https://doi.org/10.4028/www.scientific.net/AMR.382.100>
33. Okudu, K., Okamoto, H., Yoshihiro, H.: Amorphous Si polycrystalline Si stacked solar cell having more than 12% conversion efficiency. *Jpn. J. Appl. Phys.* **9**, 605–607 (1983). <https://doi.org/10.1143/JJAP.22.L605>
34. Tanaka, M., Taguchi, M., Matsuyama, T., Sawada, T., Tsuda, S., Nakano, S., Hanafusa, H., Kuwano, Y.: Development of new a-Si/C-Si heterojunction solar cells ACJ-HIT artificially constructed junction-heterojunction with intrinsic thin-layer. *Jpn. J. Appl. Phys. Part 1-Regul. Pap. Short Notes Rev. Pap.* **31**, 3518–3522 (1992). <https://doi.org/10.1143/JJAP.31.3518>
35. Benick, J., Müller, R., Schindler, F., Richter, A., Hauser, H., Feldmann, F., Krenckel, P., Riepe, S., Schubert, M.C., Hermle, M.: Approaching 22% efficiency with multicrystalline n-type silicon solar cells. *PV Sol. Energy Conf. Exhib.* **33**, 1188–1197 (2017)
36. Yoshikawa, K., Yoshida, W., Irie, T., Kawasaki, H., Konishi, K., Ishibashi, H., Asatani, T., Adachi, D., Kanematsu, M., Uzu, H., Yamamoto, K.: Exceeding conversion efficiency of 26% by heterojunction interdigitated back contact solar cell with thin film Si technology. *Sol. Energy Mater. Sol. Cells* **173**, 37–42 (2017). <https://doi.org/10.1016/j.solmat.2017.06.024>
37. Yoshikawa, K., Kawasaki, H., Yoshida, W., Irie, T., Konishi, K., Nakano, K., Uto, T., Adachi, D., Kanematsu, M., Uzu, H., Yamamoto, K.: Silicon heterojunction solar cell with interdigitated back contacts for a photoconversion efficiency over 26%. *Nat. Energy* **2**, 17032 (2017). <https://doi.org/10.1038/nenergy.2017.32>
38. Haase, F., Hollemann, C., Schäfer, S., Merkle, A., Rienäcker, M., Krügener, J., Brendel, R., Peibst, R.: Laser contact openings for local poly-Si-metal contacts enabling 26.1%-efficient POLO-IBC solar cells. *Sol. Energy Mater. Sol. Cells* **186**, 184–193 (2018). <https://doi.org/10.1016/j.solmat.2018.06.020>
39. Green, M.A., Hishikawa, Y., Dunlop, E.D., Levi, D.H., Hohl-Ebinger, J., Ho-Baillie, A.W.Y.: Solar cell efficiency tables (version 52). *Prog. Photovolt. Res. Appl.* **26**, 427–436 (2018). <https://doi.org/10.1002/ppp.3040>
40. Ali, A., Gouveas, T., Hasan, M.-a, Zaidi, S.H., Asghar, M.: Influence of deep level defects on the performance of crystalline silicon solar cells: experimental and simulation study. *Sol. Energy Mater. Sol. Cells* **95**, 2805–2810 (2011). <https://doi.org/10.1016/j.solmat.2011.05.032>
41. Aksari, M.B., Eray, A.: Optimization of a-Si:H/c-Si heterojunction solar cells by numerical simulation. *Energy Procedia* **10**, 101–105 (2011). <https://doi.org/10.1016/j.egypro.2011.10.160>
42. Oppong-Antwi, L., Huang, S., Li, Q., Chi, D., Meng, X., He, L.: Influence of defect states and fixed charges located at the a-Si:H/c-Si interface on the performance of HIT solar cells. *Sol. Energy* **141**, 222–227 (2017). <https://doi.org/10.1016/j.solener.2016.11.049>
43. Rawat, A., Sharma, M., Chaudhary, D., Sudhakar, S., Kumar, S.: Numerical simulations for high efficiency HIT solar cells using microcrystalline silicon as emitter and back surface field (BSF) layers. *Sol. Energy* **110**, 691–703 (2014). <https://doi.org/10.1016/j.solener.2014.10.004>
44. Cruz, A., Wang, E.C., Morales-Vilches, A.B., Meza, D., Neubert, S., Szyszka, B., Schlatmann, R., Stannowski, B.: Effect of front TCO on the performance of rear-junction silicon heterojunction solar cells: Insights from simulations and experiments. *Sol. Energy Mater. Sol. Cells* **195**, 339–345 (2019). <https://doi.org/10.1016/j.solmat.2019.01.047>
45. Chavali, R.V.K., Johlin, E.C., Gray, J.L., Buonassisi, T., Alam, M.A.: A framework for process-to-module modeling of a-Si/c-Si (HIT) heterojunction solar cells to investigate the cell-to-module efficiency gap. *IEEE J. Photovolt.* **6**, 875–887 (2016). <https://doi.org/10.1109/JPHOTOV.2016.2557060>
46. Zhao, L., Zhou, C.L., Li, H.L., Diao, H.W., Wang, W.J.: Design optimization of bifacial HIT solar cells on p-type silicon substrates by simulation. *Sol. Energy Mater. Sol. Cells* **92**, 673–681 (2008). <https://doi.org/10.1016/j.solmat.2008.01.018>
47. Wen, X., Zeng, X., Liao, W., Lei, Q., Yin, S.: An approach for improving the carriers transport properties of a-Si:H/c-Si heterojunction solar cells with efficiency of more than 27%. *Sol. Energy* **96**, 168–176 (2013). <https://doi.org/10.1016/j.solener.2013.07.019>
48. Singh, S., Kumar, S., Dwivedi, N.: Band gap optimization of p-i-n layers of a-Si:H by computer aided simulation for development of efficient solar cell. *Sol. Energy* **86**, 1470–1476 (2012). <https://doi.org/10.1016/j.solener.2012.02.007>
49. Stangl, R., Kriegel, M., Schmidt, M.: AFORS-HET, version 2.2, a numerical computer program for simulation of heterojunction solar cells and measurements. In: Conference on Record 2006 IEEE 4th World Conference Photovoltaic Energy Conversion, WCPEC-4. vol. 2, pp. 1350–1353 (2007). <https://doi.org/10.1109/WCPEC.2006.279681>
50. Stangl, R., Kriegel, M., Maydell, K. V., Korte, L., Schmidt, M., Fuhs, W.: AFORS-HET, an open-source on demand numerical PC program for simulation of (thin film) heterojunction solar cells, version 1.2. In: Conference Record IEEE Photovoltaic Specific Conference, pp. 1556–1559 (2005). <https://doi.org/https://doi.org/10.1109/PVSC.2005.1488441>
51. Kanneboina, V., Madaka, R., Agarwal, P.: High open circuit voltage c-Si/a-Si: H heterojunction solar cells: influence of hydrogen plasma treatment studied by spectroscopic ellipsometry. *Sol. Energy* **166**, 255–266 (2018b). <https://doi.org/10.1016/j.solener.2018.03.068>
52. Stangl, R., Leendertz, C., Haschke, J.: Numerical simulation of solar cells and solar cell characterization methods: the open-source on demand program AFORS-HET (2010)
53. Yao, Y., Xu, X., Zhang, X., Zhou, H., Gu, X., Xiao, S.: Enhanced efficiency in bifacial HIT solar cells by gradient doping with AFORS-HET simulation. *Mater. Sci. Semicond. Process.* **77**, 16–23 (2018). <https://doi.org/10.1016/j.mssp.2018.01.009>

54. Shah, A.: Thin Film Silicon Solar Cells. EPFL Press, New York (2010)
55. Antonio, H., Hegedus, S.: Handbook of Photovoltaic Science and Engineering. Wiley, New York. (2003). <https://doi.org/10.1002/9780470974704>

Publisher's Note Springer Nature remains neutral with regard to jurisdictional claims in published maps and institutional affiliations.